

Ultrafast random laser emission in a dye-doped silica gel powder

Sara García-Revilla,¹ Joaquín Fernández,^{1,2,*} Maria Asunción Illarramendi,¹ Begoña García-Ramiro,¹ Rolindes Balda,^{1,2} Hongtao Cui,³ Marcos Zayat,³ and David Levy³

¹Departamento Física Aplicada I, Escuela Técnica Superior de Ingeniería, Alda. Urquijo s/n 48013 Bilbao, Spain

²Unidad Física de Materiales CSIC-UPV/EHU and Donostia Internacional Physics Center, Apartado 1072, 20080 San Sebastián, Spain

³Instituto de Ciencia de Materiales de Madrid-ICMM, CSIC Cantoblanco, 28049 Madrid, Spain

*Corresponding author: wupferoj@bi.ehu.es

Abstract: We report efficient random lasing in a ground powder of a novel solid-state material based on silica gel containing SiO₂ nanoparticles embedding rhodamine 6G (Rh6G) dye. Basic properties of random lasing such as emission kinetics, emission spectrum, and threshold of stimulated emission are investigated by using real-time spectroscopy. The laser-like emission dynamics can be accurately described by a light diffusive propagation model. The device behavior is close to a conventional ultrafast Q-switched laser, which is an interesting fact aimed to further applications.

©2008 Optical Society of America

OCIS codes: (140.3380) Laser materials; (300.6500) Spectroscopy, time-resolved; (290.4210) Multiple scattering; (320.7090) Ultrafast lasers.

References and links

1. V. S. Letokhov, "Stimulated emission of an ensemble of scattering particles with negative absorption," *JETP Lett.* **5**, 212-215 (1967).
2. H. Cao, Y. G. Zhao, S. T. Ho, E. W. Seeling, Q. H. Wang, and R. P. H. Chang, "Random laser action in semiconductor powder," *Phys. Rev. Lett.* **82**, 2278-2281 (1999).
3. H. Cao, J. Y. Xu, S.-H. Chang, and S. T. Ho, "Transition from amplified spontaneous emission to laser action in strongly scattering media," *Phys. Rev. E* **61**, 1985-1989 (2000).
4. R. C. Polson, M. E. Raikh, and Z. V. Vardeny, "Universal properties of random lasers," *IEEE J. Sel. Top. Quantum Electron.* **9**, 120-123 (2003).
5. S. Mujumdar, V. Turck, R. Torre, and D. S. Wiersma, "Chaotic behavior of a random laser with static disorder," *Phys. Rev. A* **76**, 033807 (2007).
6. X. Wu and H. Cao, "Statistical studies of random-lasing modes and amplified spontaneous-emission spikes in weakly scattering systems," *Phys. Rev. A* **77**, 013832 (2008).
7. K. L. van der Molen, "Experiments on scattering lasers from Mie to random," (Univ. Twente, Enschede, 2007).
8. D. S. Wiersma, "The physics and applications of random lasers," *Nature Phys.* **4**, 359-367 (2008).
9. H. Cao, "Lasing in random media," *Waves Random Media* **13**, R1-R39 (2003).
10. M. A. Noginov, *Solid-State Random Lasers*, (Springer, Berlin, 2005)
11. S. John and G. Pang, "Theory of lasing in a multiple-scattering medium," *Phys. Rev. A* **54**, 3642-3652 (1996).
12. D. S. Wiersma and A. Lagendijk, "Light diffusion with gain and random lasers," *Phys. Rev. E* **54**, 4256-4265 (1996).
13. X. Jiang and C. M. Soukoulis, "Time dependent theory for random lasers," *Phys. Rev. Lett.* **85**, 70-73 (2000).
14. A. L. Burin, M. A. Ratner, H. Cao, and R. P. H. Chang, "Model for a random laser," *Phys. Rev. Lett.* **87**, 215503 (2001).
15. K. L. van der Molen, A. P. Mosk, and A. Lagendijk, "Quantitative analysis of several random lasers," *Opt. Commun.* **278**, 110-113 (2007).
16. S. Ferjani, V. Barna, A. De Luca, C. Versace, and G. Strangi, "Random lasing in freely suspended dye-doped nematic liquid crystals," *Opt. Lett.* **33**, 557-559 (2008).
17. N. M. Lawandy, R. M. Balachandran, A. S. L. Gomes, and E. Sauvain, "Laser action in strongly scattering media," *Nature* **368**, 436-438 (1994).

18. D. Anglos, A. Stassinopoulos, R. N. Das, G. Zacharakis, M. Psyllaki, R. Jakubiak, R. A. Vaia, E. P. Giannelis, and S. H. Anastasiadis, "Random laser action in organic-inorganic nanocomposites," *J. Opt. Soc. Am. B* **21**, 208-213 (2004).
19. H. Z. Wang, F. L. Zhao, Y. J. He, X. G. Zheng, X. G. Huang, and M. M. Wu, "Low-threshold lasing of a Rhodamine dye solution embedded with nanoparticle fractal aggregates," *Opt. Lett.* **23**, 777-779 (1998).
20. W. L. Sha, C. H. Liu, and R. R. Alfano, "Spectral and temporal measurements of laser action of Rhodamine 640 dye in strongly scattering media," *Opt. Lett.* **19**, 1922-1924 (1994).
21. M. Siddique, R. R. Alfano, G. A. Berger, M. Kempe, and A. Z. Genack, "Time-resolved studies of stimulated emission from colloidal dye solutions," *Opt. Lett.* **21**, 450-452 (1996).
22. G. Zacharakis, G. Heliotis, G. Filippidis, D. Anglos, and T. G. Papazoglou, "Investigation of the laserlike behavior of polymeric scattering gain media under subpicosecond laser excitation," *Appl. Opt.* **38**, 6087-6092 (1999).
23. C. W. Lee, K. S. Wong, J. D. Huang, S. V. Frolov, and Z. V. Vardeny, "Femtosecond time-resolved laser action in poly(p-phenylene vinylene) films: stimulated emission in an inhomogeneously broadened exciton distribution," *Chem. Phys. Lett.* **314**, 564-569 (1999).
24. H. W. Shin, S. Y. Cho, K. H. Choi, S. L. Oh, and Y. R. Kim, "Directional random lasing in dye-TiO₂ doped polymer nanowire array embedded in porous alumina membrane," *Appl. Phys. Lett.* **88**, 263112 (2006).
25. D. Zhang, Y. Wang, and D. Ma, "Random lasing emission from a red fluorescent dye doped polystyrene film containing dispersed polystyrene nanoparticles," *Appl. Phys. Lett.* **91**, 091115 (2007).
26. S. V. Frolov, Z. V. Vardeny, A. A. Zakhidov, and R. H. Baughman, "Laser-like emission in opal photonic crystals," *Opt. Commun.* **162**, 241-246 (1999).
27. S. Gottardo, R. Sapienza, P. D. Garcia, A. Blanco, D. S. Wiersma, and C. Lopez, "Resonance-driven random lasing," *Nature Photon.* **2**, 429-432 (2008).
28. C. J. Brinker and G. W. Sherer, *Sol-Gel Science: The Physics and Chemistry of Sol-Gel Processing*, (Academic Press, San Diego, 1990)
29. B. García-Ramiro, M. A. Illarramendi, I. Aramburu, J. Fernández, R. Balda, and M. Al-Saleh, "Light propagation in optical crystal powders: effects of particle size and volume filling factor," *J. Phys.: Condens. Matter* **19**, 456213 (2007).
30. M. A. Illarramendi, I. Aramburu, J. Fernández, R. Balda, S. N. Williams, J. A. Adegoke, and M. A. Noginov, "Characterization of light scattering in translucent ceramics," *J. Opt. Soc. Am. B* **24**, 43-48 (2007).
31. V. S. Letokhov, "Generation of light by a scattering medium with negative resonance absorption," *Sov. Phys. JETP* **26**, 835-840 (1968).
32. L. Florescu and S. John, "Lasing in a random amplifying medium: Spatiotemporal characteristics and nonadiabatic atomic dynamics," *Phys. Rev. E* **70**, 036607 (2004).
33. A. Z. Genack, "Optical transmission in disordered media," *Phys. Rev. Lett.* **58**, 2043-2046 (1987).
34. G. A. Berger, M. Kempe, and A. Z. Genack, "Dynamics of stimulated emission from random media," *Phys. Rev. E* **56**, 6118-6122 (1997).
35. G. van Soest, F. J. Poelwijk, R. Sprik, and A. Lagendijk, "Dynamics of a random laser above threshold," *Phys. Rev. Lett.* **86**, 1522-1525 (2001).
36. G. van Soest, "Experiments on Random Lasers," (Univ. Amsterdam, Amsterdam, 2001).
37. M. A. Noginov, H. J. Caulfield, N. E. Noginova, and P. Venkateswarlu, "Line narrowing in the dye solution with scattering centers," *Opt. Commun.* **118**, 430-437 (1995).
38. A. E. Siegman, *Lasers*, (Mill Valley, California, 1986)
39. R. M. Balachandran and N. M. Lawandy, "Theory of laser action in scattering gain media," *Opt. Lett.* **22**, 319-321 (1997).

1. Introduction

Light amplification in locally inhomogeneous dielectric materials is a fascinating topic that gathers fundamental aspects of both classical and quantum optics together. In 1967, Letokhov theoretically predicted the possibility of generating laser-like emission starting from scattering particles with negative absorption, the so-called *random* or *powder laser*, in which the feedback mechanism is provided by disordered-induced light scattering due to the spatial inhomogeneity of the medium [1]. The general spectral signatures of random lasing are an overall narrowing of the emission spectrum, a threshold behavior, and the eventual presence of narrow spikes in the emission spectrum. Experiments by Cao and co-workers revealed for the first time the presence of these spikes in the emission spectrum of zinc oxide powders [2]

the origin of which, also observed later in other materials [3,4], is still under discussion [5-8]. In any case, the specific feedback mechanism and behavior of a given system depend on its particular nature and morphology [9,10]. A detailed discussion about the physics of random lasers can be found in a recent publication by Wiersma [8]. The first experiments on random lasers around 1986 promoted a remarkable scientific activity in the following years when different kinds of random lasers were proposed and studied such as: neodymium, liquid dye, polymer, and ZnO based random lasers, as well as electron-beam-pumped random lasers, liquid crystal random lasers, random lasing in human tissues, etc [8-10 and references therein]. In spite of the large variety of materials and morphologies studied, random lasers are still of little practical use and lack of a satisfactory theoretical understanding. The reason could be the high degree of complexity in obtaining the required feedback which can be achieved either by the randomly dispersed scatterers or by the medium surrounding them. Moreover, the huge variety of possible dielectric properties of both media and the different packing densities which may occur, make it difficult to study all the systems with a unique theoretical treatment [11-14]. On the other hand, in order to deal with results from different experiments, much care is needed to avoid and/or to take into account the influence of the experimental conditions on the system studied, in particular, the precise way in which the sample is excited and light emission collected, as well as the influence of the boundaries imposed by the sample holder [15,16]. Unfortunately, there are only a few time-resolved random laser experiments in which all these issues are considered as well as measurements performed both in the spectral and time domains [17-23]. Moreover, within the class of dye random lasers, only a few have been conducted by embedding the dye in a solid host [22,24-27]. Keeping all these facts in mind, we present in this article a detailed real-time spectroscopic study of a new solid-state random laser based on ground powder made of silica gel containing SiO₂ nanoparticles embedding Rh6G dye. This solid-state system has a quenched disorder contrarily to liquid dye random lasers, where the organic laser dyes and external scattering particles lie in an inert matrix (solvent). Moreover, in our system the dye is embedded in the bulk of the nanoparticles and not at their surface as in the case of dye doped opals. On the other hand, in such an active ground powder the amount of scattering can be easily varied by changing the particle size in the grinding process. The main aim of this work is to show that the experimental behavior of this new developed solid-state random laser (with non-resonant feedback), can be accurately studied by using ultrafast time-resolved spectroscopy and its emission dynamics adequately explained by using a simplified rate equation-diffusion model. The temporal analysis of the light emitted above threshold by this solid-state random laser clearly suggests a behavior which is similar to a laser device working in a Q-switch-like regime. Our findings could be of much interest in the understanding of results obtained from other solid-state random lasers as well as for the development of new systems operating within the diffusive approximation.

2. Experimental

2.1 Sample preparation

The laser sample consisting of rhodamine 6G doped silica particles embedded in a silica matrix was prepared via the sol-gel method [28] in a two-step procedure. In a first stage, the Rh6G doped SiO₂ nanoparticles are synthesized. The particles are then dispersed in a silica matrix to obtain the final laser material. A detailed description of the preparation procedure is given below and schematized in Fig. 1.

The fluorescent nanoparticles were prepared by dissolving rhodamine 6G in ethanol (6.6×10^{-3} M) and the subsequent addition of tetraethoxysilane (TEOS) to obtain a Rh6G/TEOS ratio of 0.022. The solution was stirred prior to the addition of 1M ammonia solution (ammonia/Si = 0.174). The resulting mixture was vigorously stirred for one hour, and then 10 mL of 0.269M TEOS in ethanol solution were added to 17 mL of the previously prepared

solution, followed by the addition of 3.8 mL of 0.206M ammonia solution. The solution was allowed to hydrolyze under vigorous stirring and then stabilized for the precipitation of the Rh6G doped SiO₂ nanoparticles. After separation from the supernatant liquid and drying, the dye-doped particles were ready for the next step of the procedure. The measured concentration of Rh6G in the particles was 3.1 wt%.

For the preparation of the doped silica gel, 2 wt% of the previously prepared Rh6G-SiO₂ nanoparticles were dispersed in ormosil sols to form the fluorescent particles doped hybrid gel, which was finally dried at 50 °C for two weeks.

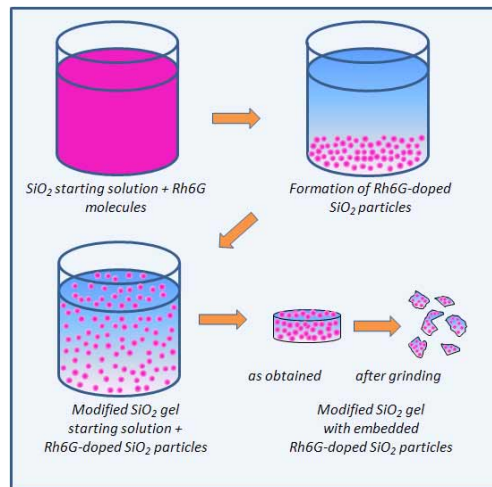


Fig. 1. Two-step preparation of Rh6G-doped silica nanoparticles embedded in a modified silica matrix.

In order to obtain ground powder out of the silica gel containing 2% Rh6G-SiO₂ nanoparticles, a mixer mill (Retsch MM200) was employed during 4 min. The polydispersity of the measured powder was evaluated from Scanning Electron Microscopy. The particle size was estimated from the average between the major and minor axis lengths of the grains. The histogram of the particle size was fitted to a log-normal function and an average powder size of $3 \pm 1.2 \mu\text{m}$ was obtained. The resulting powder was compacted in a 6 mm high cylindrical quartz cell for handling ease and optical characterization. The volume filling factor of the powder material ($f = 0.43$) was calculated by measuring sample volume and weight. Thickness dependence of diffuse transmittance was evaluated in order to experimentally determine the transport mean free path (l_t) of the ground powder [29,30]. The absolute diffuse transmittance spectra of the ground powder with less than 500 μm sample thickness were measured in a Cary 5 spectrometer with an integrated sphere assembly. On-axis transmission measurements of those samples with a larger thickness (up to 2.5 mm) were performed by exciting with a diode laser at 656 nm. In this case, the transmitted light was detected by using a photomultiplier (Hamamatsu R928) connected to a lock-in amplifier (EG&G Princeton Applied Research 5210). The estimated value of l_t was $9.5 \pm 0.5 \mu\text{m}$ for a wavelength of 656 nm.

2.2 Experimental techniques

The spectral and temporal measurements were performed at room temperature in a backscattering arrangement by using the frequency doubled output (532 nm) of a 10 Hz, Q-switched Nd: YAG laser (Continuum PY61C-10) as the excitation source (see Fig. 2). The pump pulse duration was 40 ps. The laser excitation energy was attenuated from 1.5 mJ/pulse

to 5 $\mu\text{J}/\text{pulse}$ with a pair of polarizers and measured with an energy meter (OPHIR PE10). The laser beam was impinged on the sample at normal incidence with a spot size of 2 mm after reflection from a dichroic mirror. Ground powder was compacted in a 6 mm height cylindrical cuvette with no front cell window. This sample holder has a diameter size larger than the incident laser spot (6 mm and 2 mm, respectively). The emission from the free sample surface was collected along the backward direction of the incident pump beam with an optical fiber by use of two lenses (see Fig. 2). This geometry, also used to perform temporal measurements, is particularly useful to reduce reflection effects of the pump and emitted radiation in the cuvette walls. A long-pass filter (Semrock LP532) was used to remove light at the pump frequency.

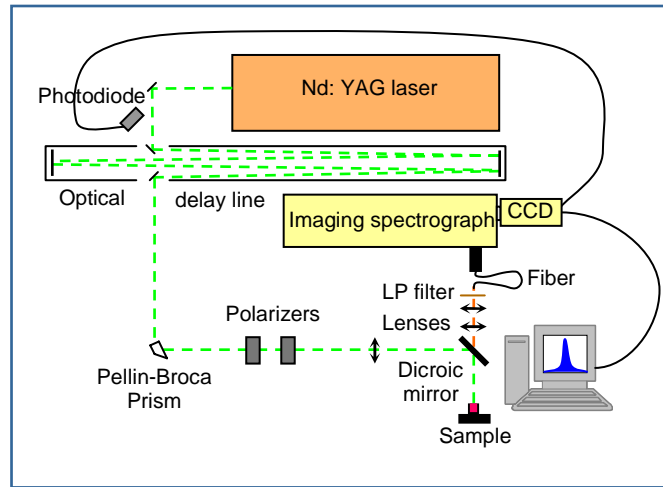


Fig. 2. Experimental set-up for time-resolved spectroscopy measurements.

In the spectral measurements, the emitted light was dispersed by a 0.5 m imaging spectrograph (Chromex 500is) equipped with three gratings of 150, 300, and 600 grooves/mm with spectral resolutions of 0.6, 0.3, and 0.15 nm, respectively. In the present work, a 150 grooves/mm grating blazed at 800 nm and a gated intensified CCD camera (Stanford Computer Optics, Inc. 4 Picos) were used. This camera allows time-resolved detection of luminescence with exposure times down to 200 ps and variable delays after excitation. Time reference was provided by a fast photodiode which monitored a small fraction of the incident laser beam. Temporal measurements were recorded by coupling the optical fiber with a fast photodiode (Thorlabs SUV7-FC) connected to a 13 GHz bandwidth digital oscilloscope (Agilent Infiniium DSA91304A). In this case, the temporal response was limited by the 100 ps detector resolution.

3. Theoretical background

Light propagation in ground powder of silica gel containing 2% Rh6G-SiO₂ nanoparticles can be described by the model of light diffusion which was proposed to be applied to random lasers in the pioneering work by Letokhov in 1968 [31]. The average particle size of our ground powder provides mean free paths in the scattering medium which are much larger than the wavelength ($l_t = 9.5 \mu\text{m}$ at 656 nm) and, consequently, the condition for the diffusion approximation is satisfied ($\lambda \ll l_t \ll L$, where L is the scattering sample thickness). This approximation has been conscientiously tested and its validity has been proven for the description of light transport [32,33]. Moreover, it has been successfully used to analyze the behavior of several random lasers [11,12,21,34,35].

At the pump and emission wavelengths ($\lambda_p = 532$ nm and $\lambda_e = 598$ nm respectively), the generalized time-dependent random laser equations describing our system are:

$$\frac{\partial W_p(z,t)}{\partial t} = D_p \frac{\partial^2 W_p(z,t)}{\partial z^2} - \frac{D_p}{l_{abs}^2} W_p(z,t) + p(z,t) \quad (1)$$

$$\frac{\partial W_e(z,t)}{\partial t} = D_e \frac{\partial^2 W_e(z,t)}{\partial z^2} + f v \sigma_{em} N(z,t) W_e(z,t) + \beta \frac{N(z,t)}{\tau_s} \quad (2)$$

$$\frac{\partial N(z,t)}{\partial t} = f v K_{abs} W_p(z,t) - f v \sigma_{em} N(z,t) W_e(z,t) - \frac{N(z,t)}{\tau_s} \quad (3)$$

where $W_{p,e}(z,t)$ are the pump and emission light densities, $N(z,t)$ is the density of the dye molecules in the excited state, $v = c/n_{eff}$ is the light speed in the medium where n_{eff} is the effective refractive index, σ_{em} is the stimulated emission cross section, τ_s is the excited state lifetime, and K_{abs} is the absorption coefficient of the material at the pump wavelength.

$l_{abs} = \sqrt{\frac{l_t l_i}{3}}$ and $D = \frac{v l_t}{3}$ are the diffusive absorption length and the light diffusion coefficient

respectively. We have distinguished the diffusion coefficients for pump and emitted radiation, D_p and D_e , respectively. The definitions of the mean free path lengths involved in the scattering and absorption processes are given elsewhere [29]. β is the fraction of spontaneous emission contributing to the laser process. The volume fraction occupied by the scatterers, f , has been included into the equations to take into account the effective part of the light density which penetrates inside the particles. This effect is not considered in most of the laser equations under the diffusion approximation given in the literature [12,35,36] but it must be regarded in order to explain the dependence of random laser threshold and efficiency on volume filling factor. Note that no reabsorption terms have been included in equations (1)-(3) due to the negligible absorption at the emission wavelength (598 nm). The source of diffuse radiation, $p(z,t)$, is a Gaussian pulse incoming the sample in the z direction which is extinguished (scattered and absorbed) along the scattering path:

$$p(z,t) = \frac{j_0}{l_s} \frac{\sqrt{\ln 2}}{\sqrt{\pi} \Delta} \exp\left(-\frac{z}{l^*}\right) \exp\left(-\left(\frac{(t-t_{peak}-z/v)}{\Delta}\right)^2 \ln 2\right) \quad (4)$$

Here, j_0 is the incident light intensity, t_{peak} is the time at which the pump pulse is maximum at the sample surface and Δ is its length half width at half maximum.

For a slab geometry in the x - y plane, the boundary conditions are $W_p(-l_e^0, t) = W_p(L+l_e^L, t) = W_e(-l_e^0, t) = W_e(L+l_e^L, t) = N(z,0) = 0$, where the extrapolation

lengths are given by $l_e^{0,L} = \frac{2h_{0,L}}{3} l_t$, with $h_{0,L} = \frac{1+r_{0,L}}{1-r_{0,L}}$. $r_{0,L}$ are the internal reflectivities at

the front ($z = 0$) and rear ($z = L$) surface. The time evolution of the reflected flux corresponding to the emitted light is given by $\bar{F}_e = -D_e \frac{\partial W_e}{\partial z} \bar{z}$ evaluated at the sample surface ($z = 0$).

4. Results and discussion

We report experimental and theoretical studies of the laser-like effects of a novel organic-inorganic hybrid material consisting of Rh6G doped SiO₂ nanoparticles embedded in a SiO₂ gel matrix. The bulk matrix is transparent at daylight, due to the rather small refractive-index mismatch between the silica gel and the Rh6G-SiO₂ nanoparticles (~10 nm diameter) so a small scattering effect is expected. Nevertheless, random laser phenomenon is possible in the opaque ground powder of this hybrid nanocomposite. As it will be shown in the following, the

dye doped silica gel powder acts as an efficient enough light scatter in the spectral range of the Rh6G optical gain. Note that in contrast to conventional liquid dye random lasers [17,20,37], no passive scatterers are required to achieve laser-like emission in our scattering active medium.

4.1 Time-resolved spectroscopies

In order to study the effect of multiple scattering on the light emitted by our silica gel containing 2% Rh6G-SiO₂ nanoparticles, spectral and temporal characteristics such as linewidth and threshold behaviors were investigated in a backscattering arrangement, both in the bulk matrix and in the resulting ground powder. Within the first set of experiments we studied the spectral characteristics of their emissions after picosecond optical pumping in single shot measurements. The emission spectra evolution for the bulk matrix and the ground powder is shown as a function of the pump pulse energy in Figs. 3a and 3b. In both cases, at low excitation energies, the emission spectra show the typical broad fluorescence band of Rh6G centered at 616 nm. However, in the ground powder sample as the pump energy is increased, a gain-narrowed peak rises centered at 598 nm (see right inset of Fig. 3(b)). At sufficiently high energies, only the gain-narrowed peak survives whereas the broad tails of the photoluminescence are completely suppressed. Left inset of Fig. 3(b) shows the effective linewidth ($\Delta\lambda_{eff} = \int \frac{I(\lambda)d\lambda}{I_{max}}$) collapse from 51.8 nm to 10.8 nm. The bulk sample, on the

other hand, shows no narrowing as a function of the pump energy, with the linewidth remaining nearly constant (see left inset of Fig. 3(a)). It is also worth mentioning the blueshift found in the stimulated emission peak of our ground powder sample at high pump pulse energies in comparison with the spontaneous emission band of Rh6G in the silica matrix (right inset of Fig. 3(b)). This spectral feature of the emission has been also previously observed in dye solutions with scatterers [17,20] and has been attributed to a change in the distribution of population of the excited state [10].

To obtain a detailed insight into the emission dynamics of our ground powder, time-resolved spectroscopy measurements were carried out around and above threshold for spectral narrowing. Figure 4(a) shows the emission spectra of the ground powder measured with a gate width of 200 ps and variable delays after excitation with 27.8 μ J single shot pulses. This pump pulse energy is close to the laser threshold (around 24 μ J/pulse) above which a suddenly drop of the spectral linewidth is observed (see inset of Fig. 3(b)). Note that time-resolved spectroscopy is the only experimental technique which allows us to separate the narrow laser-like contribution to the emission spectrum from the spontaneous emission present when exciting around the threshold. This is possible due to the different characteristic time scales involved in both processes. Figure 4(a) evidences that emission dynamics of stimulated emission is faster than that of photoluminescence.

Stimulated emission, with a maximum net gain in a narrow spectral region around 598 nm appears at the shortest time exposure and delays. At longer time delays, a broader and weaker emission band is observed (see inset of Fig. 4(a)). Both emission features are clear fingerprints of the photoluminescence contribution to the emission spectrum and show the slow response of the atomic system if compared to light transport [32]. Spontaneous emission is completely suppressed above a time delay of 1.8 ns which is in agreement with the measured lifetime of Rh6G in the bulk silica gel at low excitation energies (1.65 ns).

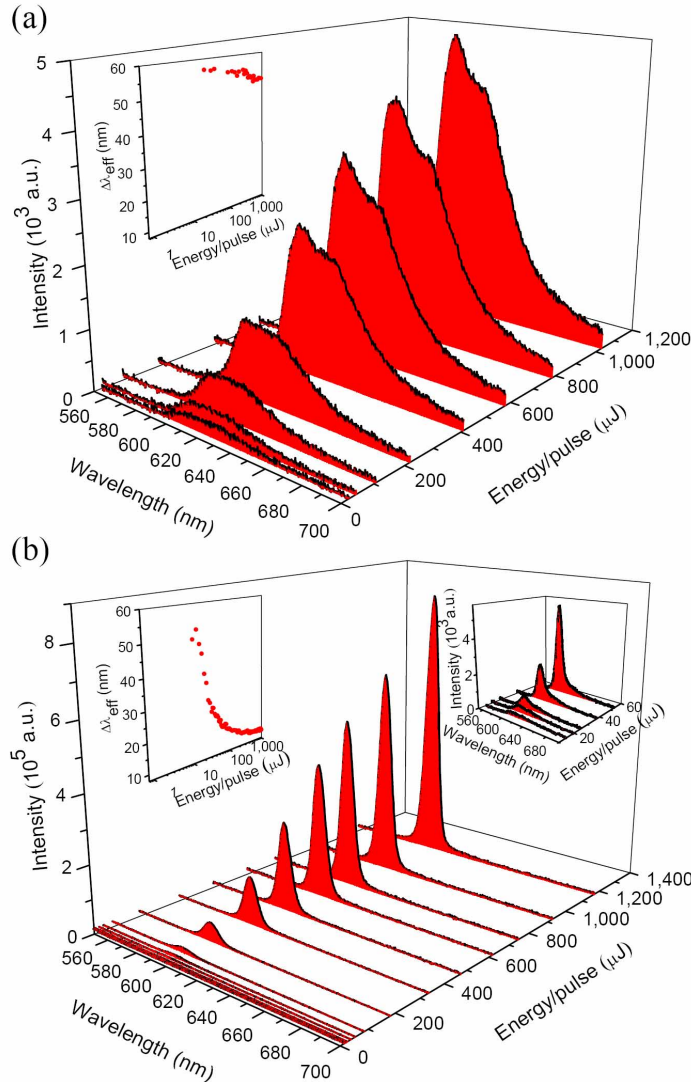


Fig. 3. Emission spectra obtained at different pump pulse energies in bulk silica gel containing 2% Rh6G-SiO₂ nanoparticles (a) and in the resulting ground powder (b). Right inset of Fig. 3(b): emission spectra of the ground powder with pump energies up to 53 $\mu\text{J}/\text{pulse}$. Left insets: corresponding emission linewidths as a function of the pump energy. Exposure times of 1.4 ns and 200 ps were used, respectively, for the bulk sample and the ground powder. The time delay employed in both cases was the same.

On the other hand, Fig. 4(b) presents the emission spectra of this sample obtained by exciting above threshold at 450 $\mu\text{J}/\text{pulse}$. At this pump energy the emission results mainly from stimulated processes and no pulsedwidth variation was thus observed as a function of time delay (see inset Fig. 4(b)). Above 0.8 ns no emission light was detected. The temporal bandwidth in which the stimulated emission spectra are observed is broader than the one found in the subsequently described temporal measurements. The reason is the temporal performance of the pico-camera (with a minimum gate width of 200 ps). It is also worthy to notice that the time delay at which the stimulated emission appears becomes shorter as pump energy is increased.

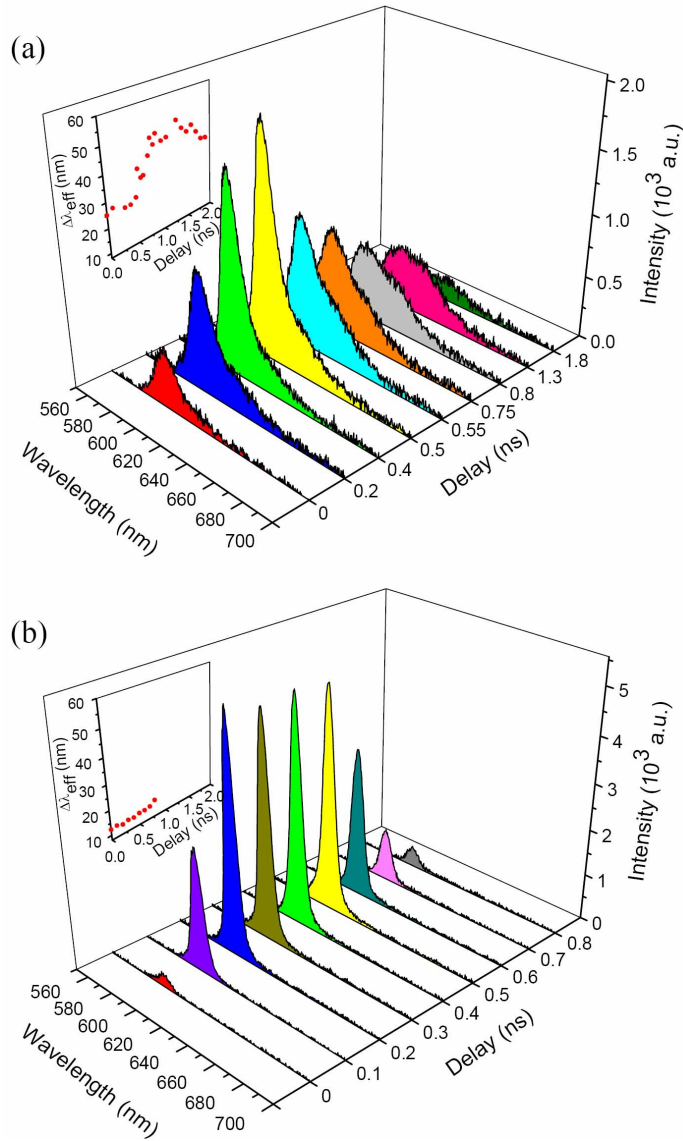


Fig. 4. Time-resolved emission spectra obtained as a function of time delay in the ground powder of a bulk silica gel containing 2% Rh6G-SiO₂ nanoparticles at 27.8 $\mu\text{J}/\text{pulse}$ energy (a) and 450 $\mu\text{J}/\text{pulse}$ energy (b). The exposure time was 200 ps in both cases. Insets: respective linewidths as a function of the pump energy.

The temporal characteristics of the pulse emitted from the silica gel containing 2% Rh6G-SiO₂ nanoparticles were also investigated by single shot measurements. Figures 5(a) and 5(b) show the time profiles of the emission decay for the bulk matrix and the ground powder as a function of the pump pulse energy. In the former case, the emission is mainly spontaneous, resulting in an output pulse duration limited by the natural lifetime of the Rh6G dye in the silica host. This explains the almost constant full width at half maximum (FWHM) of the time profile, depicted in the inset of Fig. 5(a), as pump energy was increased. In contrast, a marked shortening of the output pulse upon crossing the threshold is observed in the ground powder.

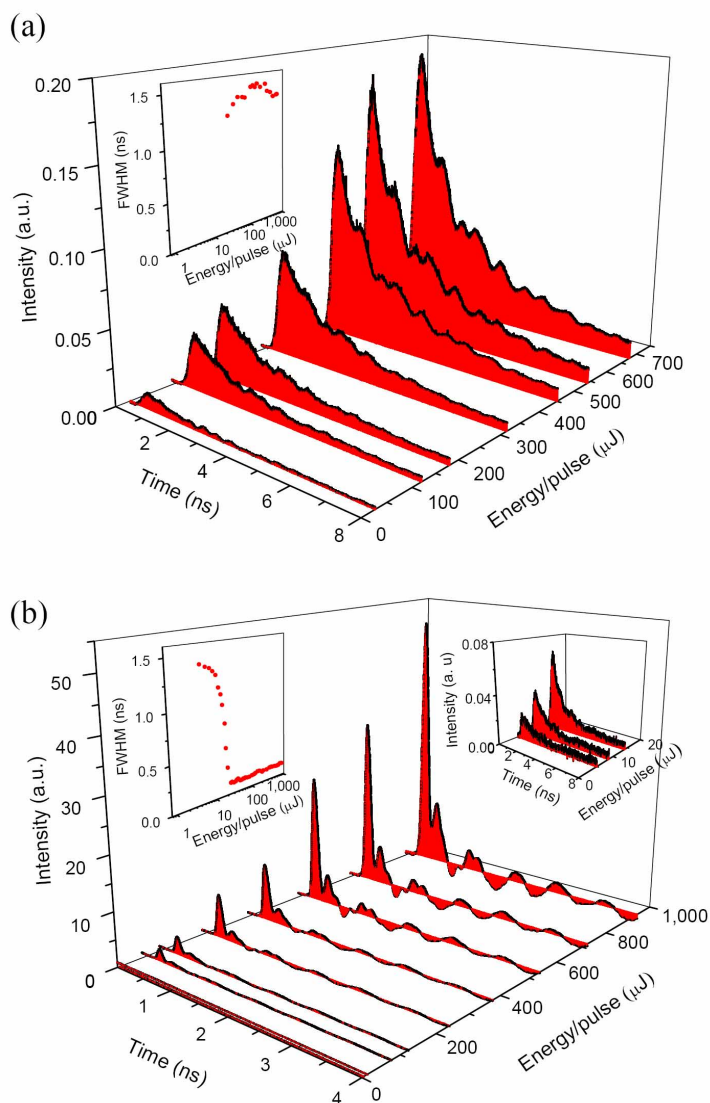


Fig. 5. Experimental temporal profiles obtained at different pump pulse energies in a bulk silica gel containing 2% Rh6G-SiO₂ nanoparticles (a) and in the resulting ground powder (b). Right inset of Fig. 5(b): temporal profiles of the ground powder with pump energies up to 14 $\mu\text{J}/\text{pulse}$. Note the different time scale in this case. The wavy structure of the temporal profiles is due to the typical response of the fast photodiode used in the experimental set-up. Left insets: FWHM of the respective time profiles as a function of the pump energy. Note that in the powder sample the width of the temporal profiles is reduced down to 100 ps which corresponds to the actual detector system resolution.

Right inset of Fig. 5(b) shows the corresponding time profiles up to 14 $\mu\text{J}/\text{pulse}$ energy, below the onset of laser-like action, where the emission exhibits the characteristic nanosecond decay profile of the Rh6G spontaneous emission. When the pump pulse energy is beyond the threshold level, the pulse profile becomes strongly shortened to a pulse in the subnanosecond range (see Fig. 5(b) and notice that time scale ranges from 0 to 4 ns). Left inset of Fig. 5(b) shows the resulting sharp FWHM drop of the output pulse as a function of pump energy. This figure evidences that the pulse duration was reduced down to around 100 ps which is the

actual time resolution of the detector we used to perform these temporal measurements. Note that the 40 ps excitation pulses give also the same time-width, so it is rather possible that our real temporal width be much narrower. As a matter of fact, studies on liquid dye and polymer sheet random lasers have given emission pulses as short as 50 ps [22] or even less [20,21].

As a conclusion, the experimental data presented in Figs. 3(b) and 5(b) clearly show parallel behaviors in spectral and time domains as a function of the pumping energy, demonstrating that: (1) Below the threshold energy, the ground powder of the silica gel containing 2% Rh6G-SiO₂ nanoparticles exhibits the same emission features as the bulk matrix. (2) On the contrary, above threshold the spectral and temporal narrowing only occurs in the ground powder. (3) It is worthy to notice that spikes were not observed in the single shot emission spectra of the ground powder at high pump pulse energies even when using the grating with the best spectral resolution (0.15 nm). This experimental fact could indicate that no light path inside the sample has enough gain for spikes to occur.

Finally, a good photostability under VIS laser pulse irradiation was proven by using 100 μJ pump pulse energy. Almost no change in the integrated emission intensity was observed after an irradiation time of two hours.

4.2 Modeling

The theoretical calculations on light diffusion with amplification have been performed by using the laser model described in Sec. 3. The set of coupled nonlinear partial differential equations has been numerically solved by the Crank-Nicholson finite difference method ($\Delta z = 0.05 \mu\text{m}$, $\Delta t = 10 \text{ ps}$). The input values for the calculation are the material parameters: $\sigma_{em} = 2.5 \times 10^{-16} \text{ cm}^2$, $\tau_s = 1.65 \text{ ns}$, $K_{abs}(532 \text{ nm}) = 148.5 \text{ cm}^{-1}$, $n_{eff} = 1.16$, $f = 0.43$ and $t_{peak} = 120 \text{ ps}$ and $\Delta = 20 \text{ ps}$. The effective refractive index has been calculated by using the Maxwell-Garnet theory. The mean free paths at the required wavelengths ($\lambda_p = 532 \text{ nm}$ and $\lambda_e = 598 \text{ nm}$) have been calculated by using the Mie theory for spheres in the independent-scatterer approximation with a diameter equal to the averaged mean particle size ($\phi = 3 \mu\text{m}$). In spite of the fact that this material can be closely-packed, the effect of the spatial correlations on scattering and absorption processes can be neglected [29]. The obtained values for the mean free paths are: $l_s = 2 \mu\text{m}$, $l_t = 8.9 \mu\text{m}$, $l_{abs} = 21.6 \mu\text{m}$, $l^* = 2.0 \mu\text{m}$ at 532 nm, and $l_t = 9 \mu\text{m}$ at 598 nm. The value for l_t calculated from this theory at 656 nm agrees with the one experimentally obtained from the dependence on the sample thickness of the diffuse transmittance. This proves the Mie theory is reliable in order to predict the mean free paths in our scattering medium. The average internal reflectivities of the sample have been estimated from the Fresnel reflection coefficients by using the effective refractive index of the random system [29,30] ($r_o = 0.24$ and $r_L = 0.3$).

Figure 6 shows the excited-state populations (blue curves) and the temporal profiles of the emitted light (red lines) obtained as a function of the pump pulse energy. As it was expected, a dramatic pulse shortening is obtained when the excitation energy is increased. Note that in this case, the time scale ranges from 0 to just 0.4 ns. The right inset of Fig. 6 depicts the corresponding excited-state populations and time profiles obtained up to 36.5 μJ/pulse energy. In the left inset of Fig. 6 the pulse duration predicted by our model is plotted against the excitation energy. The change in FWHM with pump energy, from 1.31 ns to 12 ps, can be reliably used to theoretically determine the threshold energy where narrowing takes place [22,36], leading to a theoretical threshold of 24 μJ/pulse.

Figure 7(a) compares the theoretically predicted pulse shortening (left inset of Fig. 6) with the experimentally determined one in the ground powder (left inset of Fig. 5(b)). In the latter, error bars are also included. Although the experimental pulse width is limited by the actual time resolution of the detector, and, therefore a larger experimental pulse duration is obtained at high energies, the FWHM collapses around the same energy value in both cases. The slightly broader experimental output pulses measured below threshold may be due to reabsorption of the emitted light.

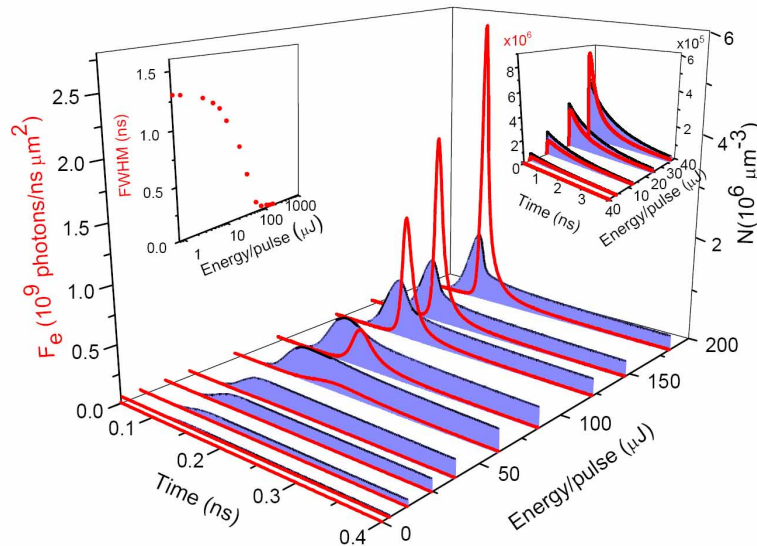


Fig. 6. Theoretical temporal behavior obtained at different pump pulse energies. Blue curves represent the excited-state populations and red lines correspond to the time profiles obtained for $\beta = 0.5$ at the same pump pulse energy value. Right inset: excited-state populations and simulated temporal profiles obtained for pump energies up to $36.5 \mu\text{J}/\text{pulse}$. Note the different time scale in this case. Left inset: FWHM of the simulated time profiles as a function of the pump pulse energy.

It is worthy to mention that the build-up of the laser-like emitted pulse can be interpreted in the framework of ordinary Q-switch laser theory account taken of the formal similarity between our “laser equations” (see Sec. 3) and the ones proposed by Florescu & John [32]. Moreover, following ref. [32], our equations can be reduced to the basic Q-switch laser equations $\frac{dW_e}{dt} = v\sigma_{em}NW_e - \gamma_c W_e$, $\frac{dN}{dt} \approx -2v\sigma_{em}W_e N$ during the pulse build-up time [38]. Here, W_e is the photon density, N the population difference density, and γ_c the “cavity” decay rate which is related to the diffusion coefficient, D_e , by $\gamma_c \equiv D_e / l_z^2$, where $l_z \cong 3l_{abs}$ [35,39]. A “cavity” decay time $\tau_c = 1/\gamma_c$ of 5.5 ps is thus obtained for our system. This value is close to the one given by the Q-switch theory, 6.4 ps, obtained from the time-dependence of N around the threshold and the output pulse width [38] (see Fig. 6).

Figure 7(b) shows the integrated intensity of the output pulses measured as a function of the input pump energy in the ground powder (red dots). A laser threshold around $24 \mu\text{J}/\text{pulse}$ is clearly observed from the linear fit of the experimental data. This value is in good agreement with the theoretical estimation of the laser threshold given above. The solid curve in Fig. 7(b) results from numerical integrations of the theoretical temporal profiles for $\beta = 0.5$ (blue line). In the theoretical model, β is the fraction of spontaneous emission contributing to the laser process and describes the sharpness of the laser threshold. Note that the theoretically calculated input-output curve perfectly follows the experimental behavior of our ground powder (red dots, Fig. 7(b)).

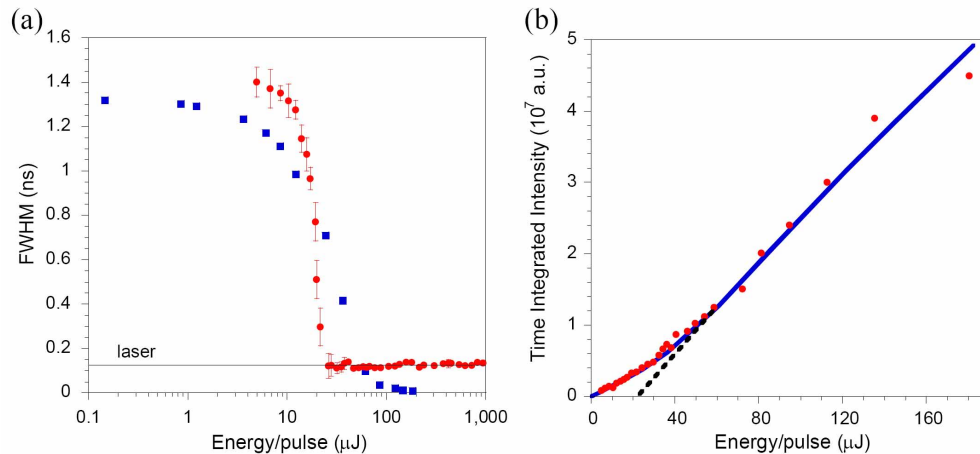


Fig. 7(a) Theoretical (blue squares) and experimental (red dots) pulse narrowing obtained as a function of the pump pulse energy in the ground powders of the bulk silica gel containing 2% Rh6G-SiO₂ nanoparticles. The horizontal line represents the FWHM of the pump pulse indicating the actual detector system resolution. (b) Integrated intensity of the corresponding temporal profiles as a function of the pump pulse energy. Blue line represents the simulated data for $\beta = 0.5$. A laser threshold around 24 $\mu\text{J}/\text{pulse}$ is estimated from the linear fit (dashed line) of the experimental data (red dots)

5. Conclusions

We have presented a detailed experimental study of the emission dynamics in a novel solid-state random laser fabricated by the sol-gel technique. This laser system based on scattering gain media is obtained by grinding a silica gel containing 2% Rh6G-SiO₂ nanoparticles. Random laser-like effects such as spectral narrowing, emission intensity increase, and pulse shortening have been observed for the first time in ground powder of such kind of organic-inorganic nanocomposites above 24 $\mu\text{J}/\text{pump pulse}$. We have clearly demonstrated that within diffusive conditions of light propagation, a laser model with feedback provided by the ground powder is able to describe the laser-like emission features successfully. In particular, both good qualitative and quantitative agreements between the experimental and theoretical results are obtained for the pulse duration collapse and laser threshold. The behavior of our system is close to a classical Q-switched laser under ultrashort pump.

Based on the ease of material fabrication, processability, and good photostability, we believe that the present hybrid disordered material opens up the possibility of using a dye doped powder as an alternative source for a photonic device utilizing random lasing phenomenon.

Acknowledgments

Funding for this research is provided by the Spanish Government MEC under Projects No. MAT2008-05921/MAT, NAN2004-09317-C04-02 and Consolider CSD2007-00013. S. G.-R. acknowledges financial support from the Spanish MEC under the “Juan de la Cierva” program. The authors are grateful to Dr. M. Al-Saleh for his assistance and to Prof. M.A. Arriandiaga for useful discussions.